

Tree-ring ^{14}C links seismic swarm to CO_2 spike at Yellowstone, USA

William C. Evans^{1*}, Deborah Bergfeld¹, John P. McGeehin², John C. King³, and Henry Heasler⁴

¹U.S. Geological Survey, 345 Middlefield Road, Menlo Park, California 94025, USA

²U.S. Geological Survey, 12201 Sunrise Valley Drive, Reston, Virginia 20192, USA

³Lone Pine Research, 2604 Westridge Drive, Bozeman, Montana 59715, USA

⁴National Park Service, Yellowstone National Park, Wyoming 82190, USA

ABSTRACT

Mechanisms to explain swarms of shallow seismicity and inflation-deflation cycles at Yellowstone caldera (western United States) commonly invoke episodic escape of magma-derived brines or gases from the ductile zone, but no correlative changes in the surface efflux of magmatic constituents have ever been documented. Our analysis of individual growth rings in a tree core from the Mud Volcano thermal area within the caldera links a sharp $\sim 25\%$ drop in ^{14}C to a local seismic swarm in 1978. The implied fivefold increase in CO_2 emissions clearly associates swarm seismicity with upflow of magma-derived fluid and shows that pulses of magmatic CO_2 can rapidly traverse the 5-km-thick brittle zone, even through Yellowstone's enormous hydrothermal reservoir. The 1978 event predates annual deformation surveys, but recognized connections between subsequent seismic swarms and changes in deformation suggest that CO_2 might drive both processes.

INTRODUCTION

Plants that grow in areas of strong magmatic CO_2 emissions fix carbon that is depleted in ^{14}C relative to normal atmosphere, and annual records of emission strength can be preserved in tree rings (Marzaioli et al., 2005). Tree-ring ^{14}C showed that the onset and peak of CO_2 efflux at Mammoth Mountain volcano (California, United States) closely followed a 1989 seismic swarm attributed to dike intrusion (Cook et al., 2001). Perhaps due to uncertainty over site selection, tree-ring ^{14}C studies had not been attempted at Yellowstone caldera (Wyoming, United States), even though delineating the sources of unrest at this giant caldera is key to the assessment of hazards. Yellowstone is a logical target because its swarm seismicity and deformation are often ascribed to buildup and escape of high-pressure magmatic fluids (Fournier, 1989; Dzurisin et al., 1994; Waite and Smith, 2002), including CO_2 (Husen et al., 2004). The youngest lavas within the 640 ka caldera erupted 70 ka, but the ongoing unrest and the presence of sizable Holocene explosion craters in this popular national park drive a volcano monitoring program that includes a focus on fluid discharges (Christiansen et al., 2007; Lowenstern and Hurwitz, 2008; Hurwitz et al., 2007). An estimated 10,000 hot springs, geysers, and fumaroles are widely scattered in and around the 2500 km² caldera, but are mostly concentrated into a few dozen major thermal areas (Fournier, 1989; Werner and Brantley, 2003).

MUD VOLCANO AND 1978 SEISMIC SWARM

The Mud Volcano thermal area is smaller than many other Yellowstone thermal areas, but is located close to the point of maximum uplift of the caldera floor (~ 72 cm) that occurred between 1923 and 1976 (Pelton and Smith, 1979), and discharges gas with the highest, most magmatic $^3\text{He}/^4\text{He}$ ratios in the park (Werner and Brantley, 2003; Kennedy et al., 1985). The thermal area comprises ~ 30 separate hydrothermal features consisting of fumaroles, gassy pools, and mudpots, plus several zones where CO_2 issues diffusely through the soil (Fig. 1). A rigorous investigation of CO_2 emissions at Mud Volcano thermal area in 1997 found a total CO_2 output of 380 ± 100 t/day from diffuse and discrete vent sources covering a 0.4 km² area (Werner et al., 2000a).

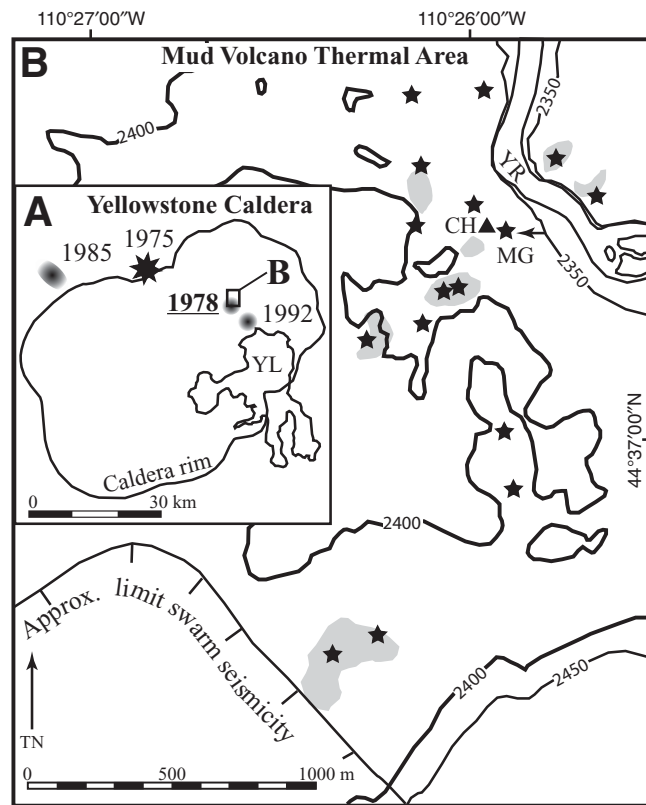


Figure 1. A: Yellowstone caldera, notable seismic swarms (stippled), and M 6.1 event (star) from Dzurisin et al. (1994). YL—Yellowstone Lake. B: Mud Volcano thermal area, major thermal features (stars), 1979 tree-kill areas (gray—from Pitt and Hutchinson, 1982), and study tree (triangle). YR—Yellowstone River; MG—Mud Geyser; CH—Cooking Hillside. Small arrow shows camera location in Figure 2.

The 7 month seismic swarm that began in May 1978 was centered near the southwest end of the thermal area (Fig. 1A) and was notable for the large number of earthquakes, at times reaching 100 events per hour (Pitt and Hutchinson, 1982). As is typical of most intracaldera seismicity at Yellowstone, hypocenters ranged from ~ 1 km down to 5 km, the approximate depth of the brittle-ductile transition zone (Fournier, 1989; Dzurisin et al., 1994; Waite and Smith, 2002; Husen et al., 2004). Clear signs of increased heat output followed the seismic swarm (Pitt and Hutchinson, 1982). Rising soil temperatures began killing trees, primarily lodgepole pine (*Pinus contorta* Douglas ex Louden), at the southwest end of the thermal area in December 1978, and new mudpots and fumaroles formed between January and May 1979 as existing features increased in activity. Large areas of increased soil temperature and tree mortality appeared throughout the 2-km-long thermal area by July 1979. The hydrothermal activity then began to decline and returned to normal levels during the winter of 1979–1980.

Pitt and Hutchinson (1982) recognized the widespread heat increase as anomalous even for Yellowstone, where the vigor and location of

*E-mail: wcevans@usgs.gov.

thermal features routinely change, and they proposed a link between the seismic activity and increased fluid upflow. However, the source and identity of the fluid could not be constrained due to the largely meteoric origin of the acid-sulfate water and steam discharged at the surface. The possible involvement of magmatic CO₂ in this event led us to test the tree-ring technique here.

TREE SELECTION AND SAMPLING

Trees in areas of strongest emissions are often selected for physiological studies that focus on nutrient uptake or stomatal conductance (Tercek et al., 2008; Sharma and Williams, 2009). However, we were careful to avoid trees that might record only the variable output of a single vent. We chose a mature, 16-m-tall lodgepole pine located 60 m from the nearest hydrothermal feature (Mud Geyser) but surrounded by 8 major hydrothermal features within a 300 m radius (Fig. 1B). This tree should, over the course of a growing season, preserve an integrated signal of emissions from a significant part of the Mud Volcano thermal area, in the same way that a 3-m-high eddy covariance tower deployed at Mud Volcano in 1999 was found to integrate surface emissions from a 350 m fetch (Werner et al., 2000b). We also verified by accumulation chamber measurements that the study tree was at least 30 m away from areas of anomalous diffuse CO₂ emission in order to avoid a potential decline in signal as the tree simply grew taller.

The study tree (CHS-C) is located in a part of the thermal area called Cooking Hillside and is an isolated survivor of the ground heating in 1979, plus later, more local episodes of kill in the 1980s and early 1990s that felled its remaining neighbors within a 50 m radius (Fig. 2). Tree-ring samples for ¹⁴C analysis were collected from CHS-C and a nearby

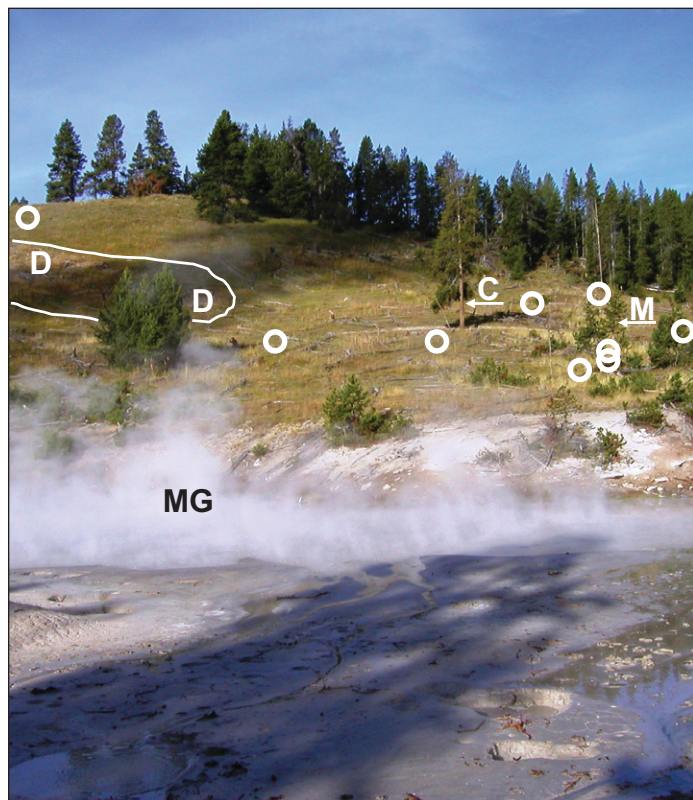


Figure 2. Cooking Hillside and 16-m-tall study tree (C), young 3.5-m-tall cored tree (M), nearest area of diffuse CO₂ emissions (D), and Mud Geyser (MG) thermal feature in foreground. Circles show fallen trees sampled for date of death.

young, 3.5-m-tall lodgepole pine (CHS-M) using 12-mm-diameter increment borers. Several 5-mm-diameter chronology development cores and an archive core were collected from each tree. Transverse sections were collected from surrounding dead, fallen trees. To develop a local record of ambient background atmospheric ¹⁴C levels during the post-1950 period of nuclear weapons testing (“bomb” pulse), as well as to eliminate any method-dependent bias, we also collected cores from a mature tree (BGT) in the southwest part of caldera, far from any sites of CO₂ emission.

SAMPLE PROCESSING AND ANALYSIS

Exact calendar year dating was established by measuring annual ring sequences to 0.001 mm accuracy and subjecting the samples and measurement series to direct comparison, graphical, and statistical cross-dating techniques. Additional confirmation was obtained by cross-dating the samples against two new lodgepole pine chronologies located within 1.5 km of the study site (filed as WY035 by J. King and W. Evans and WY036 by J. King and M.T. Tercek and accepted at the International Tree-Ring Data Bank at the World Data Center for Paleoclimatology; <http://www.ncdc.noaa.gov/paleo/treering.html>), and by a light latewood marker year in 1965. Individual annual rings were excerpted microscopically using a razor knife, ensuring no adherence of wood tissues from adjacent rings. Annual rings were processed using an acid-alkali-acid-bleach pretreatment to remove contaminant carbon that may have formed more recently than the cellulose. The pretreated wood was combusted to CO₂ and reduced to pure C as graphite on an Fe catalyst. The graphite-coated Fe was pressed into targets, which were analyzed for ¹⁴C at the Lawrence Livermore Center for Accelerator Mass Spectrometry or the National Science Foundation–Arizona Accelerator Mass Spectrometry Laboratory. A CO₂ split was analyzed for δ¹³C, and ¹⁴C values were normalized according to convention (Stuiver and Polach, 1977). Because CO₂ constitutes a large but variable fraction of the gas emitted at Mud Volcano (Werner and Brantley, 2003), the concentration of magmatic CO₂ in air (C_{mag}) was calculated using the simple formula from Sharma and Williams (2009): $C_{mag} = C_{amb}({}^{14}\text{C-BGT}/{}^{14}\text{C-CHS} - 1)$, where ¹⁴C-BGT and ¹⁴C-CHS are ¹⁴C values of the background and Cooking Hillside tree rings, respectively, and C_{amb} is the ambient background atmospheric CO₂ concentration during the year of ring growth from Keeling et al. (2009).

RESULTS

Measured ¹⁴C and calculated C_{mag} values are given in Table DR1 in the GSA Data Repository.¹ The ¹⁴C record in BGT closely tracks but is on average 1.0% higher than published (Hua and Barbetti, 2004) atmospheric ¹⁴C levels of the Northern Hemisphere Zone 1 “bomb” curve (Fig. 3A). Every ring analyzed from CHS-C is strongly depleted in ¹⁴C relative to BGT, reflecting a long and continuing history of CO₂ emission in the Mud Volcano thermal area. Similarity of ¹⁴C in the 16-m-tall CHS-C and 3.5-m-tall CHS-M trees for year 2005 shows relatively uniform C_{mag} over this range of canopy heights, ruling out a significant age-related bias in the CHS-C record. The record shows that C_{mag} in the air at canopy height was fairly stable through the early to mid-1970s, but began to rise in 1978, the year of swarm seismicity (Fig. 3B). The 1979 ring shows that C_{mag} had jumped approximately fivefold by the time of maximum surface heating, and the spike in CO₂ emissions persisted into the 1980 growing season after surface conditions had visually returned to normal.

Although the study tree is near areas of tree kill mapped in 1979, none of 11 fallen trees we examined (Fig. 2) died before 1981, and most died between 1987 and 1991 in small, isolated episodes of kill. Neither

¹GSA Data Repository item 2010296, Table DR1, CO₂ isotopes and concentrations, is available online at www.geosociety.org/pubs/ft2010.htm, or on request from editing@geosociety.org or Documents Secretary, GSA, P.O. Box 9140, Boulder, CO 80301, USA.

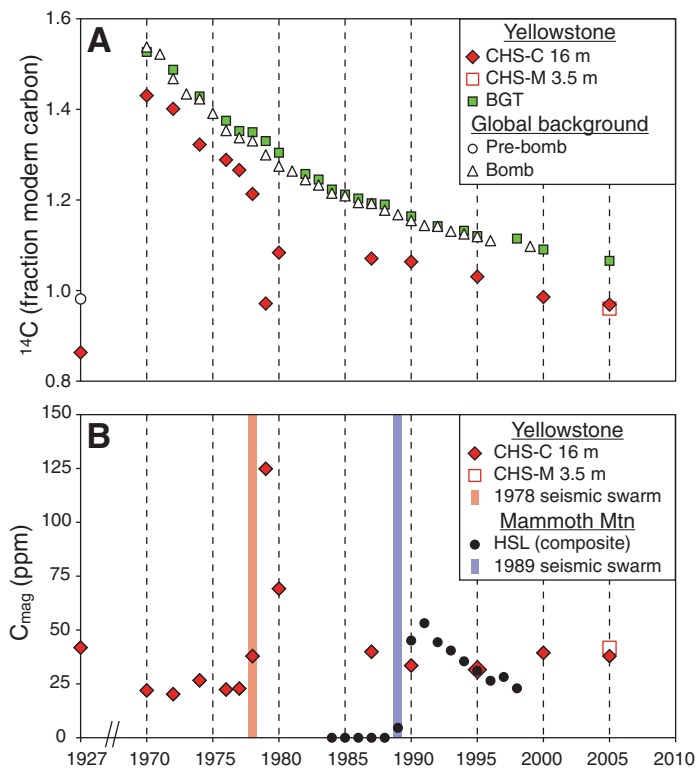


Figure 3. A: ^{14}C levels in annual rings from Cooking Hillside trees (CHS-C, CHS-M) compared to background tree (BGT) and average growing season (May–August) values from Northern Hemisphere Zone 1 “bomb” curve (Hua and Barbetti, 2004). Pre-bomb (1927) background is from Reimer et al. (2004); for supplemental data, see <http://www.radiocarbon.org/IntCal04.htm>. **B:** Concentration of magmatic CO_2 in air at Cooking Hillside calculated from depletion in ^{14}C relative to background BGT for 1970–2005, pre-bomb for 1927. Composite record from three trees near Horseshoe Lake (HSL) at Mammoth Mountain volcano (Cook et al., 2001) is shown for comparison.

these episodes nor the dramatic reawakening of the Mud Geyser feature in 1993–1995 and resultant tree kill around its margin left obvious signs in the C_{mag} record. Its insensitivity to such localized, minor events provides crucial evidence that the C_{mag} record is an integrator of CO_2 emissions from the broader Mud Volcano thermal area. The record shows no effect from the M 6.1 earthquake 15 km away in 1975, the strongest earthquake to strike within the park in the past 50 yr (Waite and Smith, 2002). The 1978–1980 spike is a unique feature of this record that links the 1978 seismic swarm to a major outpouring of CO_2 .

CO_2 -DRIVEN SEISMICITY

If we assume that the C_{mag} record from CHS-C exactly mirrors CO_2 emissions from the entire Mud Volcano thermal area, and total emissions were near 380 t/day in the late 1990s (Werner et al., 2000a), then CO_2 output likely reached ~ 1000 t/day in 1979 (Fig. 3B). This output is comparable to the peak emission rate estimated for Mammoth Mountain volcano (Cook et al., 2001; Farrar et al., 1995). At both locations, the big jump in CO_2 emissions occurred within 1–2 yr of seismic swarms. These similarities are relevant because a detailed reanalysis of the 1989 Mammoth Mountain seismic sequence, originally considered a dike intrusion, instead attributed the shallow (<6 km) seismicity to upflow of CO_2 -rich fluid escaping from magma that remained at greater depth (Hill and Prejean, 2005). Thus the CO_2 pulse at Mud Volcano was apparently large enough, and the upflow rate fast enough, to trigger swarm seismicity.

For all of Yellowstone National Park, the total efflux of CO_2 that derives from magma is huge and estimated at $\sim 45,000$ t/day, though this total may include some CO_2 released from marine-carbonate host rocks (Werner and Brantley, 2003). The total discharge of hot water from Yellowstone’s ~ 350 °C hydrothermal reservoir, corrected for boiling and surface dilution, is estimated as $\sim 300,000$ t/day (Fournier, 1989). However, δD and $\delta^{18}\text{O}$ data and chloride mass balance show that magma-derived water constitutes at most a few percent of the reservoir fluid, most of which is of meteoric origin (Fournier, 1989). These totals imply that CO_2 proportionally exceeds water in the magma-derived fluid input to the reservoir, at least on average.

The reservoir fluid is thought to be near vapor saturation (Lowenstern and Hurwitz, 2008) and incapable of dissolving much more gas. A transient jump in CO_2 leakage from the ductile zone would thus be an instant source of overpressure at the bottom of the otherwise hydrostatically pressured reservoir, capable of reducing effective normal stress and promoting slip on the numerous faults that border the Mud Volcano thermal area (Pitt and Hutchinson, 1982). Given phase relations appropriate for the reservoir (Lowenstern and Hurwitz, 2008), and the fact that CO_2 remains relatively nonreactive down to ~ 270 °C (Bischoff and Rosenbauer, 1996), consequent upflow into cooler temperature regimes could produce a self-propagating pulse of overpressure, consistent with the depth-distributed swarm seismicity. The CO_2 pulse clearly began to reach the surface concomitant with the seismic swarm during the growing season of 1978 (Fig. 3B), while increased steam discharge and surface heating began months later, perhaps as a result of permeability enhancements in the zone of seismicity. The pulse persisted into 1980 after thermal effects subsided. This sequence of events supports the concept of CO_2 -driven seismicity (Hill and Prejean, 2005; Miller et al., 2004) over alternatives such as enhanced boiling and degassing of reservoir fluid caused by seismic fracturing of near-surface rocks. That scenario would likely lead to contemporaneous pulses of gas and heat.

CALDERA DYNAMICS AND HAZARDS

The steep decline in CO_2 emissions between 1979 and 1980 (Fig. 3B) supports the view (Fournier, 1989) that open fractures seal rapidly at temperatures ≥ 350 °C and contrasts with the gradual decline in low-temperature CO_2 emissions at Mammoth Mountain, where upflow paths created by the 1989 seismic swarm apparently retained permeability much longer. The emissions spike at Mud Volcano may have been brief enough that any associated deflation was missed by Yellowstone leveling surveys in 1976 and 1984, which show net caldera inflation (Dzurisin et al., 1994). Still, the rapid transfer of CO_2 from ductile to brittle regimes, as suggested by the CHS-C record, might produce the pressure changes involved in deformation.

Whether CO_2 leakage and upflow ever occur at a large enough scale to cause caldera-wide deformation at Yellowstone is of great interest because uplift and deflation might then be temporally independent of intrusion and drainage of magma. The CHS-C record shows no definitive effects from a decade of rapid deflation that began in 1985 or the subsequent return to uplift. Values of C_{mag} remain slightly higher after the spike than before it, but no higher than the value recorded by the innermost 1927 ring. The decade of deflation has been putatively linked to fluid escape during later seismic swarms in 1985 and 1992 (Fig. 1) located ~ 40 and 7 km, respectively, from Mud Volcano (Dzurisin et al., 1994; Waite and Smith, 2002; Husen et al., 2004). If CO_2 escape during either swarm caused the deflation, the CHS-C record implies that a strong ^{14}C signal should be detectable through additional tree coring, possibly with a focus on trees closer to the locations of these later swarms. A weak ^{14}C signal or one restricted solely to the epicentral regions, while providing additional evidence of CO_2 -driven seismicity, might favor mechanisms that link

inflation-deflation cycles to movement of magma (Wicks et al., 2006; Chang et al., 2007) or some process other than CO₂ escape.

Within the Campi Flegrei of Italy, gas measurements at Solfatara have found higher CO₂ emissions during cyclical inflation (Chiodini et al., 2003; Caliro et al., 2007). This observation has helped constrain the relative roles of magma intrusion, fluid movement, and poroelastic expansion in the deformation of that caldera (Rinaldi et al., 2010), and aided the evaluation of hazards. A more complete record of CO₂ emissions could serve the same purpose at Yellowstone. Techniques now exist for continuous monitoring of CO₂ emissions. Some monitoring is currently conducted by park staff at Yellowstone, where asphyxia kills numerous types of animals including birds that enter pit depressions within several of the thermal areas. Tree-ring ¹⁴C studies, in addition to testing the link between emissions and historic periods of deformation, can reveal the large natural variability in CO₂ emission strength to be expected in areas accessible to the public.

ACKNOWLEDGMENTS

We thank C. Hendrix, S. Gunther, C. Jaworowski, and C. Curry of the U.S. National Park Service for logistical help and access to park archives. Suggestions, comments, or reviews from J. Lowenstern, D. Dzurisin, S. Hurwitz, M. Pitt, C. Newhall, and two anonymous reviewers are greatly appreciated. George Burr (University of Arizona) advised on ¹⁴C data formats.

REFERENCES CITED

- Bischoff, J.L., and Rosenbauer, R.J., 1996, The alteration of rhyolite in CO₂ charged water at 200 and 350°C: The unreactivity of CO₂ at higher temperatures: *Geochimica et Cosmochimica Acta*, v. 60, p. 3859–3867, doi: 10.1016/0016-7037(96)00208-6.
- Caliro, S., Chiodini, G., Moretti, R., Avino, R., Granieri, D., Russo, M., and Fiebig, J., 2007, The origin of the fumaroles of La Solfatara (Campi Flegrei, south Italy): *Geochimica et Cosmochimica Acta*, v. 71, p. 3040–3055, doi: 10.1016/j.gca.2007.04.007.
- Chang, W.L., Smith, R.B., Wicks, C., Farrell, J.M., and Puskas, C.M., 2007, Accelerated uplift and magmatic intrusion of the Yellowstone caldera, 2004 to 2006: *Science*, v. 318, p. 952–956, doi: 10.1126/science.1146842.
- Chiodini, G., Todesco, M., Caliro, S., Del Gaudio, C., Macedonio, G., and Russo, M., 2003, Magma degassing as a trigger of bradyseismic events: The case of Phlegrean Fields (Italy): *Geophysical Research Letters*, v. 30, 1434, 4 p., doi: 10.1029/2002GL016790.
- Christiansen, R.L., Lowenstern, J.B., Smith, R.B., Heasler, H., Morgan, L.A., Nathenson, M., Mastin, L.G., Muffler, L.J.P., and Robinson, J.E., 2007, Preliminary assessment of volcanic and hydrothermal hazards in Yellowstone National Park and vicinity: U.S. Geological Survey Open-File Report 2007–1071, 94 p.
- Cook, A.C., Hainsworth, L.J., Sorey, M.L., Evans, W.C., and Southon, J.R., 2001, Radiocarbon studies of plant leaves and tree rings from Mammoth Mountain, CA: A long-term record of magmatic CO₂ release: *Chemical Geology*, v. 177, p. 117–131, doi: 10.1016/S0009-2541(00)00386-7.
- Dzurisin, D., Yamashita, K.M., and Kleinman, J.W., 1994, Mechanisms of crustal uplift and subsidence at the Yellowstone caldera, Wyoming: *Bulletin of Volcanology*, v. 56, p. 261–270, doi: 10.1007/BF00302079.
- Farrar, C.D., Sorey, M.L., Evans, W.C., Howle, J.F., Kerr, B.D., Kennedy, B.M., King, C.-Y., and Southon, J.R., 1995, Forest-killing diffuse CO₂ emission at Mammoth Mountain as a sign of magmatic unrest: *Nature*, v. 376, p. 675–678, doi: 10.1038/376675a0.
- Fournier, R.O., 1989, Geochemistry and dynamics of the Yellowstone National Park hydrothermal system: *Annual Review of Earth and Planetary Sciences*, v. 17, p. 13–53, doi: 10.1146/annurev.earth.17.050189.000305.
- Hill, D.P., and Prejean, S., 2005, Magmatic unrest beneath Mammoth Mountain, California: *Journal of Volcanology and Geothermal Research*, v. 146, p. 257–283, doi: 10.1016/j.jvolgeores.2005.03.002.
- Hua, Q., and Barbetti, M., 2004, Review of tropospheric bomb ¹⁴C data for carbon cycle modeling and age calibration purposes: *Radiocarbon*, v. 46, p. 1273–1298.
- Hurwitz, S., Lowenstern, J.B., and Heasler, H., 2007, Spatial and temporal geochemical trends in the hydrothermal system of Yellowstone National Park: Inferences from river solute fluxes: *Journal of Volcanology and Geothermal Research*, v. 162, p. 149–171, doi: 10.1016/j.jvolgeores.2007.01.003.
- Husen, S., Smith, R.B., and Waite, G.P., 2004, Evidence for gas and magmatic sources beneath the Yellowstone volcanic field from seismic tomographic imaging: *Journal of Volcanology and Geothermal Research*, v. 131, p. 397–410, doi: 10.1016/S0377-0273(03)00416-5.
- Keeling, R.F., Piper, S.C., Bollenbacher, A.F., and Walker, S.J., 2009, Atmospheric CO₂ values (ppmv) derived from in situ air samples collected at Mauna Loa, Hawaii, USA: <http://cdiac.ornl.gov/ftp/trends/co2/maunaloa.co2> (June 2009).
- Kennedy, B.M., Lynch, M.A., Reynolds, J.H., and Smith, S.P., 1985, Intensive sampling of noble gases in fluids at Yellowstone, I. Early overview of the data, regional patterns: *Geochimica et Cosmochimica Acta*, v. 49, p. 1251–1261, doi: 10.1016/0016-7037(85)90014-6.
- Lowenstern, J.B., and Hurwitz, S., 2008, Monitoring a supervolcano in repose: Heat and volatile flux at the Yellowstone caldera: *Elements*, v. 4, p. 35–40, doi: 10.2113/GSELEMENTS.4.1.35.
- Marzaioli, F., Lubritto, C., Battipaglia, G., Passariello, I., Rubino, M., Rogalla, D., Strumia, S., Miglietta, F., D’Onofrio, A., Cotrufo, M.F., and Terrasi, F., 2005, Reconstruction of past CO₂ concentration at a natural CO₂ vent site using radiocarbon dating of tree rings: *Radiocarbon*, v. 47, p. 257–263.
- Miller, S.A., Collettini, C., Chiaraluce, L., Cocco, M., Barchi, M., and Kaus, B.J.P., 2004, Aftershocks driven by a high-pressure CO₂ source at depth: *Nature*, v. 427, p. 724–727, doi: 10.1038/nature02251.
- Pelton, J.R., and Smith, R.B., 1979, Recent crustal uplift in Yellowstone National Park: *Science*, v. 206, p. 1179–1182, doi: 10.1126/science.206.4423.1179.
- Pitt, A.M., and Hutchinson, R.A., 1982, Hydrothermal changes related to earthquake activity at Mud Volcano, Yellowstone National Park, Wyoming: *Journal of Geophysical Research*, v. 87, p. 2762–2766, doi: 10.1029/JB087iB04p02762.
- Reimer, P.J., and 28 others, 2004, IntCal04 terrestrial radiocarbon age calibration, 0–26 cal kyr BP: *Radiocarbon*, v. 46, p. 1029–1058.
- Rinaldi, A.P., Todesco, M., and Bonafede, M., 2010, Hydrothermal instability and ground displacement at the Campi Flegrei caldera: *Physics of the Earth and Planetary Interiors*, v. 178, p. 155–161, doi: 10.1016/j.pepi.2009.09.005.
- Sharma, S., and Williams, D.G., 2009, Carbon and oxygen isotope analysis of leaf biomass reveals contrasting photosynthetic responses to elevated CO₂ near geologic vents in Yellowstone National Park: *Biogeosciences*, v. 6, p. 25–31, doi: 10.5194/bg-6-25-2009.
- Stuiver, M., and Polach, H.A., 1977, Discussion: Reporting of ¹⁴C data: *Radiocarbon*, v. 19, p. 355–363.
- Tercek, M.T., Al-Niemi, T.S., and Stout, R.G., 2008, Plants exposed to high levels of carbon dioxide in Yellowstone National Park: A glimpse into the future?: *Yellowstone Science*, v. 16, p. 12–19.
- Waite, G.P., and Smith, R.B., 2002, Seismic evidence for fluid migration accompanying subsidence of the Yellowstone caldera: *Journal of Geophysical Research*, v. 107, B92177, doi: 10.1029/2001JB000586.
- Werner, C., and Brantley, S., 2003, CO₂ emissions from the Yellowstone volcanic system: *Geochemistry, Geophysics, Geosystems*, v. 4, 1061, doi: 10.1029/2002GC000473.
- Werner, C., Brantley, S.L., and Boomer, K., 2000a, CO₂ emissions related to the Yellowstone volcanic system 2. Statistical sampling, total degassing, and transport mechanisms: *Journal of Geophysical Research*, v. 105, p. 10,831–10,846, doi: 10.1029/1999JB900331.
- Werner, C., Wyngaard, J.C., and Brantley, S.L., 2000b, Eddy-correlation measurement of hydrothermal gases: *Geophysical Research Letters*, v. 27, p. 2925–2928.
- Wicks, C.W., Thatcher, W., Dzurisin, D., and Svarc, J., 2006, Uplift, thermal unrest and magma intrusion at Yellowstone caldera: *Nature*, v. 440, p. 72–75, doi: 10.1038/nature04507.

Manuscript received 28 April 2010

Revised manuscript received 29 June 2010

Manuscript accepted 1 July 2010

Printed in USA